



Injectable and porous PLGA microspheres that form highly porous scaffolds at body temperature



Omar Qutachi^a, Jolanda R. Vetsch^b, Daniel Gill^c, Helen Cox^c, David J. Scurr^a, Sandra Hofmann^b, Ralph Müller^b, Robin A. Quirk^c, Kevin M. Shakesheff^a, Cheryl V. Rahman^{a,*}

^aSchool of Pharmacy, University of Nottingham, University Park, Nottingham NG7 2RD, UK

^bInstitute for Biomechanics, ETH Zurich, Vladimir-Prelog-Weg 3, 8093 Zurich, Switzerland

^cRegenTec Ltd, Biocity Nottingham, Pennyfoot Street, Nottingham NG1 1GF, UK

ARTICLE INFO

Article history:

Received 21 February 2014

Received in revised form 19 July 2014

Accepted 15 August 2014

Available online 23 August 2014

Keywords:

PLGA

Microsphere

Scaffold

Porosity

Cell delivery

ABSTRACT

Injectable scaffolds are of interest in the field of regenerative medicine because of their minimally invasive mode of delivery. For tissue repair applications, it is essential that such scaffolds have the mechanical properties, porosity and pore diameter to support the formation of new tissue. In the current study, porous poly(DL-lactic acid-co-glycolic acid) (PLGA) microspheres were fabricated with an average size of $84 \pm 24 \mu\text{m}$ for use as injectable cell carriers. Treatment with ethanolic sodium hydroxide for 2 min was observed to increase surface porosity without causing the microsphere structure to disintegrate. This surface treatment also enabled the microspheres to fuse together at 37°C to form scaffold structures. The average compressive strength of the scaffolds after 24 h at 37°C was $0.9 \pm 0.1 \text{ MPa}$, and the average Young's modulus was $9.4 \pm 1.2 \text{ MPa}$. Scaffold porosity levels were 81.6% on average, with a mean pore diameter of $54 \pm 38 \mu\text{m}$. This study demonstrates a method for fabricating porous PLGA microspheres that form solid porous scaffolds at body temperature, creating an injectable system capable of supporting NIH-3T3 cell attachment and proliferation in vitro.

© 2014 Acta Materialia Inc. Published by Elsevier Ltd. This is an open access article under the CC BY-NC-ND license (<http://creativecommons.org/licenses/by-nc-nd/3.0/>).

1. Introduction

The use of polymer scaffolds to deliver cells for regenerative medicine applications can potentially overcome poor cell engraftment and improve cell survival [1]. In particular, injectable scaffolds show promise for this application, as cells can be mixed homogeneously with the scaffold formulation prior to injection. The ability to deliver injectable scaffolds in a minimally invasive manner to a cavity of any size or shape renders them especially attractive for clinical use in tissue repair. A number of synthetic polymers have been investigated for this application to date, including the biodegradable polymer poly(DL-lactic acid-co-glycolic acid) (PLGA). PLGA is frequently used in regenerative medicine applications, as the degradation rate of the polymer can be controlled and it has FDA approval for certain clinical applications [2,3]. PLGA-based scaffold systems have been reported extensively to support cell attachment and proliferation, deliver growth factors in a controlled manner, and support bone regeneration in vivo [4–8].

In order to maintain, induce and restore biological functions, scaffolds for tissue repair require suitable physical properties. Ideally, the scaffold should be strong enough to retain its structure without exhibiting stiffness that may affect the surrounding tissue [2]. The microstructural properties of the scaffold also play a vital role in successful tissue repair, as porosity levels and pore diameter influence cell attachment, proliferation and migration in addition to nutrient delivery and waste removal [9,10]. Studies have indicated that scaffolds should possess multi-scale porosity involving both micro-porosity and macro-porosity, with pore diameters ranging from $<20 \mu\text{m}$ to $>100 \mu\text{m}$ [9]. The versatility of chemically synthesized polymers such as PLGA is an advantage in this respect, as it enables the fabrication of scaffolds with different porosities and mechanical properties. However, a delicate balance is required in terms of these properties, as increasing the porosity of a scaffold causes a subsequent decrease in mechanical properties such as compressive strength. Attaining suitable porosity and strength in an injectable formulation is therefore a considerable challenge.

One type of injectable scaffold for tissue engineering applications involves the use of discreet polymer microspheres. Microspheres can be fabricated using a variety of different biodegradable polymers such as chitosan, gelatin and PLGA, and

* Corresponding author.

E-mail address: cheryl.rahman@nottingham.ac.uk (C.V. Rahman).

their use for delivery of cells and growth factors for repair of tissues such as bone, skin and brain has been reported [11–15]. Building on this strategy, microspheres with surface porosity have started to attract interest in the regenerative medicine field. Cell viability, proliferation and differentiation have been shown to be enhanced with porous microsphere systems in comparison with non-porous microspheres [16,17]. This is most likely due to the pores facilitating improved diffusion of nutrients and oxygen. A number of studies have been reported on the fabrication of porous microspheres using various natural and synthetic polymers, in addition to inorganic materials such as tricalcium phosphate [16,18–20]. Techniques employed to induce porosity during microsphere fabrication include salt-leaching or using a porogen such as gelatin [19,20]. Although such porous microspheres are injectable and provide micro-porosity, they are unable to fuse together at body temperature and therefore remain as discrete microspheres *in vivo*. This is a drawback for their use in regeneration of certain tissues such as bone, as they lack the required porosity profile and mechanical properties to support tissue repair.

The current study describes the development of an injectable, porous PLGA scaffold that solidifies *in situ* at 37 °C. A procedure for fabricating hollow, porous PLGA microspheres is described, where the microspheres were treated with ethanolic sodium hydroxide (EtOH–NaOH) to increase the surface porosity. The EtOH–NaOH treatment enables the microspheres to fuse together at 37 °C into solid scaffolds. The scaffold mechanical properties, porosity and ability to support cell attachment and proliferation were characterized *in vitro* in order to determine their suitability for use in tissue repair applications.

2. Materials and methods

2.1. Fabrication of porous microspheres

Porous PLGA microspheres were produced by the double emulsion method from 20% (w/v) P_{DL}PLGA 50:50 (52 kDa, Evonik Industries, USA) in dichloromethane (DCM, Fisher, UK). One gram of PLGA was dissolved in 5 ml DCM for each batch of microspheres. For the primary emulsion, 250 µl of the porogen (phosphate buffered saline (PBS); Gibco, UK) was added to the PLGA/DCM, and the PLGA/DCM/PBS was homogenized at 9000 rpm for 2 min using a Silverson L5M homogenizer. The primary water in oil (w/o) emulsion was then homogenized in 0.3% polyvinyl alcohol (PVA; Sigma-Aldrich, UK) at 3000 rpm and the resultant water-in-oil-in-water (w/o/w) double emulsion was left stirring overnight to allow DCM evaporation. The hardened microspheres were then harvested via distilled water (DW) washing and centrifugation.

2.2. NaOH treatment of porous microspheres

Porous PLGA microspheres were treated with ethanolic sodium hydroxide with 30% 0.25 M NaOH (Sigma-Aldrich):70% absolute ethanol (EtOH; Fisher, UK) [12]. This method was chosen because ethanol is a water-miscible solvent that partially dissolves PLGA and NaOH improves polyester surface wettability by promoting carboxylic acid exposure on the polymer surface, making it more hydrophilic [21,22]. One gram of microspheres was suspended in 10 ml of EtOH–NaOH solution with agitation on a plate rocker for 2 min, 3.5 min or 5 min, then poured onto a 50-µm sieve and rinsed with DW before transferring to a 50-ml centrifuge tube and centrifuged at 1400 rpm for 1 min. This wash and centrifugation step with DW was repeated prior to drying in a freeze-drier (Modulyo, Thermo Electron Corporation, UK) for 24 h.

2.3. Scanning electron microscopy

Microspheres were mounted on aluminium stubs (Agar Scientific, UK) and gold-coated using a Balzers SCD030 gold sputter coater (Balzers Union Ltd., Lichtenstein) with an argon rate of 30 mA for 3 min. The structural morphology of the microspheres was examined by scanning electron microscopy (SEM), using a JEOL 6060L imaging system (JEOL Ltd., Hertfordshire, UK) at 10 kV.

2.4. Microsphere size analysis

The mean microsphere diameter and size distribution were investigated using a Coulter LS230 particle size analyser (Beckman, UK). The microsphere size distribution was then determined as a function of the microsphere diffraction and plotted as a function of volume percentage.

2.5. Microsphere pore diameter analysis

The microsphere pore diameter was measured using Image J software. One hundred pore diameters were measured per image from three separate SEM images from three different batches of microspheres before and after treatment with EtOH–NaOH for 2 min.

2.6. Scaffold formation

Triplicate scaffolds were prepared in PTFE moulds producing cylindrical scaffolds 6 mm in diameter and 12 mm high. Microspheres were mixed manually with Dulbecco's Modified Eagle's Medium (DMEM; Gibco UK) using a spatula at a ratio of 1:1 (microspheres to DMEM). The resulting paste was packed into the holes of the mould, and the mould was transferred to a sealed humidified chamber containing DMEM at 37 °C. For mechanical testing experiments, moulds were transferred to a sealed humidified chamber containing DMEM at 37 °C, 40 °C and 50 °C for 24 h. After 24 h, all scaffolds were removed from the moulds. Scaffolds for micro-computed tomography (µCT) and SEM assessment were freeze-dried for 24 h and refrigerated until use.

2.7. Mechanical testing

The compressive strength of the scaffolds fabricated using sintered microspheres was tested using a TA.HD+ texture analyser (Stable Microsystems, UK) following the ASTM standard D-1621. Scaffolds were tested with the Peltier unit heated to 37 °C and a scaffold contact area of 28.3 mm². A 50-kg load cell was used for compression testing. The test speed was set at 0.04 mm s⁻¹. The mechanical testing was performed on triplicate scaffolds sintered at 37 °C for 6 h and 24 h at 37 °C, 40 °C and 50 °C. A fracture point was not observed during compression of the scaffolds, therefore the compressive strength was measured at 20% strain to compare the strength after incubating at different temperatures. The stress–strain curve generated during compression analysis was used to calculate the Young's modulus (elastic modulus) as a measure of the stiffness of the scaffolds. The elastic modulus was calculated by determining the slope of the stress–strain curve along the elastic portion of deformation.

2.8. µCT

µCT was performed on dry scaffolds in air on a µCT 40 (Scanco Medical, Brütisellen, Switzerland). Scans were performed at an energy level of 45 kVp, an intensity of 177 µA, integration time of 200 ms and a frame averaging of 4, with a nominal resolution of 6 µm. The reconstructed files were Gaussian filtered applying a

filter support of 1 voxel and filter width of sigma = 0.8. A volume of interest 400 voxels (2.4 mm) in diameter and 500 voxels (3.0 mm) high was chosen for the evaluation. Resulting greyscale images were thresholded at a global threshold of 3.3% of the maximal grey value. Objects smaller than 40 voxels were removed using component labelling and neglected for further evaluation. The resulting three-dimensional (3-D) volumes were evaluated as described previously for scaffold porosity, pore diameter distribution and average pore diameter [23,24].

2.9. Mouse 3T3 fibroblast cell culture

NIH-3T3 fibroblast cells were cultured in DMEM medium (Gibco, UK) supplemented with 10% foetal calf serum, 1% antibiotic/antimycotic solution, 1% L-glutamine (2 mM) and 1% non-essential amino acids (Sigma-Aldrich, UK). RFP-NIH-3T3 cells were previously genetically labelled with red fluorescent protein as described by Dixon and colleagues [25]. RFP-MIH-3T3 cells were cultured in the same media as NIH-3T3. All cells were maintained in a humidified tissue-culture incubator at 37 °C and with 5% CO₂.

2.10. Cell seeding on scaffolds

For scaffolds fabricated in the presence of cells, microspheres were mixed manually with DMEM (Gibco UK) containing 2×10^5 NIH-3T3 fibroblasts using a spatula at a ratio of 1:1 (microspheres to DMEM). The resulting paste was packed into the holes of the mould, and the mould was transferred to a sealed humidified chamber containing DMEM at 37 °C. After 24 h at 37 °C, all scaffolds were removed from the moulds, transferred into 12-well cell culture plates with fresh medium (1 ml per well) and incubated at 37 °C.

2.11. Cell viability assay

The PrestoBlue cell viability assay (Invitrogen Life Sciences, UK) was performed on day 3, 6 and 9 post-seeding on four scaffolds per time point. Each scaffold was submerged in 1 ml of media, and 111 µl of Prestoblue was added to each well. The scaffolds were then incubated at 37 °C for 25 min. Three 100-µl media samples were taken from each well and were read on a Tecan plate reader with the excitation wavelength set to 535 nm and the emission wavelength set at 615 nm.

2.12. Toluidine blue staining

Toluidine blue (Sigma-Aldrich, UK) staining was performed on day 7 post-seeding on triplicate scaffolds. Each scaffold was washed twice with DW and fixed in formalin solution (Sigma-Aldrich, UK) for 5 min at room temperature. Each scaffold was then washed twice in DW, and 1% toluidine blue was added to each well for 5 min at room temperature. Finally, the scaffolds were washed five times in DW and visualized under a light microscope.

2.13. Statistical analysis

Statistical analysis was performed using GraphPad Prism (Version 3) analysis software. Differences among groups were determined by ANOVA Tukey–Kramer Multiple Comparisons Test and were considered to be significantly different if $p < 0.05$.

3. Results

3.1. Fabrication of porous PLGA microspheres

PLGA microspheres were fabricated using a double emulsion process as described in Section 2.1 (Fig. 1A). Microspheres with surface porosity were generated using PBS in the internal aqueous phase during the fabrication process, as shown in Fig. 1B. Pore diameters were enlarged through treatment with EtOH–NaOH, as described in Section 2.2, which degraded the surface layer of the PLGA microspheres (Fig. 1C–E). Different lengths of time of surface treatment with EtOH–NaOH were assessed (2 min, 3.5 min and 5 min). Increased porosity compared with non-treated microspheres was observed in the SEM images. However, treating the microspheres for 3.5 or 5 min resulted in signs of structural damage to the microspheres such as cracks on the surface and disintegration of the microspheres (Fig. 1D, E). Microsphere diameter was measured as described in Section 2.4, using triplicate batches of non-treated microspheres and microspheres treated with EtOH–NaOH for 2, 3.5 and 5 min. The microsphere size distribution was similar for each batch of microspheres regardless of treatment time (Fig. 2). The average diameter of non-treated microspheres was $81 \pm 26 \mu\text{m}$, and the average diameter of treated porous microspheres was $84 \pm 24 \mu\text{m}$, $81 \pm 24 \mu\text{m}$ and $82 \pm 24 \mu\text{m}$ for 2, 3.5 and 5 min treatment, respectively (Fig. 2). In order to avoid the possibility of over-treatment with EtOH–NaOH and structural damage to the microspheres, a treatment time of 2 min was selected for porous microsphere fabrication. Microsphere pore diameters were measured before and after EtOH–NaOH treatment for 2 min, as described in Section 2.5. Pore diameters were $6 \pm 2 \mu\text{m}$ on average before treatment, with a maximum pore diameter of 9 µm. Following EtOH–NaOH treatment, pore diameters were $8 \pm 3 \mu\text{m}$ on average, with a maximum of 15 µm.

3.2. Scaffold formation using porous PLGA microspheres

Porous microspheres were packed into a PTFE mould and incubated at 37 °C for 24 h both before and after EtOH–NaOH treatment, as described in Section 2.6. Microspheres treated with EtOH–NaOH for 2 min formed solid scaffold structures over 24 h at 37 °C, as shown in Fig. 3A. SEM images show the microspheres fusing together to create the scaffold structure (Fig. 3B, C). Microspheres that were not treated with EtOH–NaOH did not fuse together over 24 h at 37 °C (Fig. 3D). As shown in Fig. 3E and F, treatment with EtOH–NaOH for 3.5 or 5 min allowed the microspheres to fuse. However, deformation of microsphere structure and collapse of pores could be visualized in these scaffolds, particularly when microspheres were treated with EtOH–NaOH for 5 min prior to scaffold fabrication. Therefore, the treatment time of 2 min was selected to produce scaffolds for further analysis in terms of their mechanical and microstructural properties. As non-treated microspheres did not form scaffolds, resulting in loose microspheres being removed from the mould after this time, a non-treated microsphere group was not included in the further studies described herein, as these were performed on whole scaffolds.

3.3. Mechanical properties of scaffolds fabricated with porous PLGA microspheres

The compressive strength and Young's modulus of scaffolds prepared with porous microspheres was assessed using a texture analyser, as described in Section 2.7. The microspheres were fabricated with PLGA that has a glass transition temperature (T_g) of ~ 50 °C. The EtOH–NaOH treated PLGA microspheres were

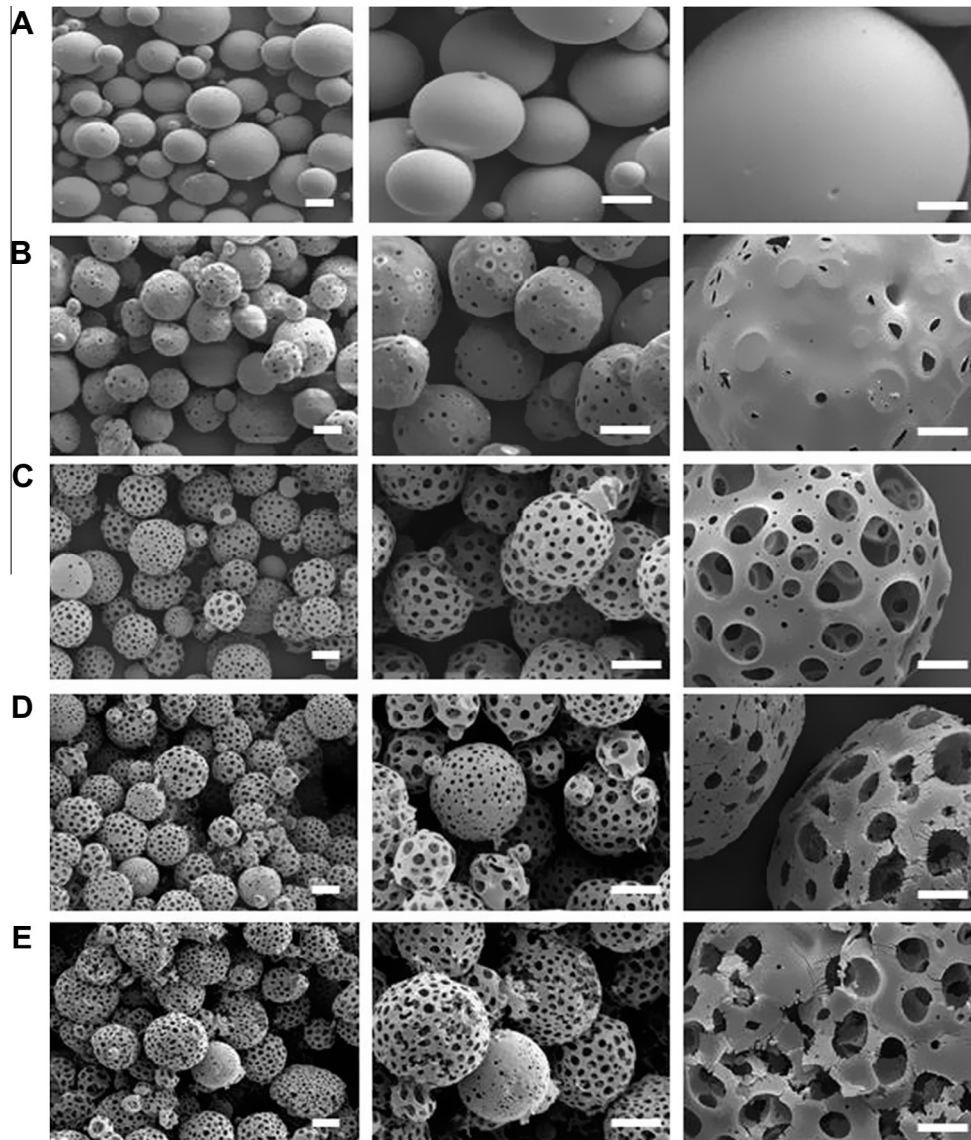


Fig. 1. Fabrication of porous PLGA microspheres. SEM micrographs of PLGA microspheres: (A) non-porous PLGA microspheres fabricated using a double emulsion process without the use of a porogen; (B) porous PLGA microspheres fabricated using a double emulsion process with PBS as a porogen (untreated); (C) porous PLGA microspheres treated for 2 min with EtOH–NaOH; (D) porous PLGA microspheres treated for 3.5 min with EtOH–NaOH; (E) porous PLGA microspheres treated for 5 min with EtOH–NaOH (scale bars represent 100 μm on left and middle images, 5 μm on right images).

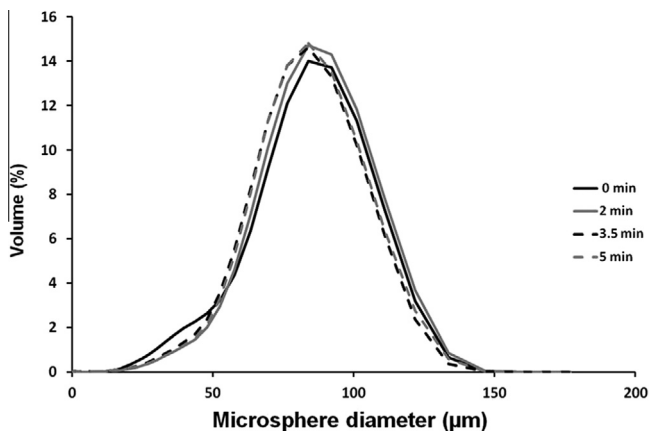


Fig. 2. Representative size distribution of porous PLGA microspheres treated with EtOH–NaOH for 0 min (black line) 2 min (grey line), 3.5 min (dashed black line) and 5 min (dashed grey line).

incubated at a range of temperatures (21 $^{\circ}\text{C}$, 37 $^{\circ}\text{C}$, 40 $^{\circ}\text{C}$ and 50 $^{\circ}\text{C}$) to investigate the effect of EtOH–NaOH treatment on the particles at these temperatures. At 21 $^{\circ}\text{C}$, the microspheres did not fuse together after the 6 h or 24 h time period, whereas at 37 $^{\circ}\text{C}$, 40 $^{\circ}\text{C}$ and 50 $^{\circ}\text{C}$, the particles fused into solid scaffold structures. As shown in the representative stress–strain graph for scaffolds formed over 24 h (Fig. 4A), a fracture point was not observed during compression of the scaffolds, therefore the compressive strength was measured at 20% strain to compare the strength after incubating at different temperatures for 6 h and 24 h (Fig. 4B). For both incubation times, the compressive strength values increased from 37 $^{\circ}\text{C}$ to 50 $^{\circ}\text{C}$. Average compressive strength for scaffolds incubated for 6 h was 0.38 ± 0.03 MPa at 37 $^{\circ}\text{C}$, 1.02 ± 0.04 MPa at 40 $^{\circ}\text{C}$ and 3.6 ± 0.7 MPa at 50 $^{\circ}\text{C}$. The average increased after 24 h to 0.9 ± 0.1 MPa at 37 $^{\circ}\text{C}$, 1.9 ± 0.3 MPa at 40 $^{\circ}\text{C}$ and 6.6 ± 1.2 MPa at 50 $^{\circ}\text{C}$.

Similar results were observed for the Young's modulus of the scaffolds from 37 $^{\circ}\text{C}$ to 50 $^{\circ}\text{C}$, as shown in Fig. 4C, with values

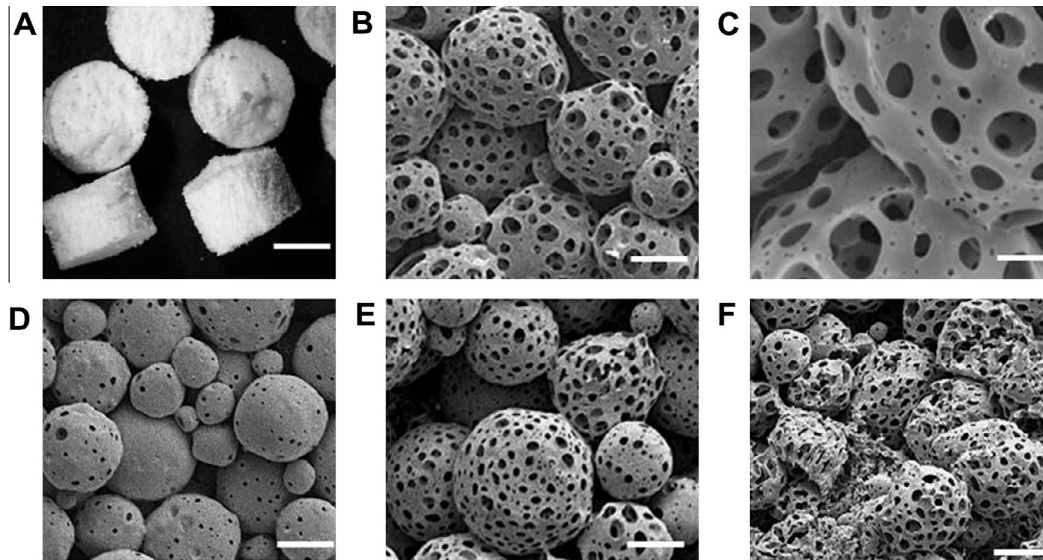


Fig. 3. Scaffolds fabricated from porous PLGA microspheres. (A) Photographic image and (B, C) SEM micrographs of a scaffold prepared with microspheres treated for 2 min with EtOH–NaOH. (D) Scaffold prepared with microspheres treated for 0 min with EtOH–NaOH (non-treated). (E) Scaffold prepared with microspheres treated for 3.5 min with EtOH–NaOH (non-treated). (F) Scaffold prepared with microspheres treated for 5 min with EtOH–NaOH (non-treated). All scaffolds were fabricated at 37 °C for 24 h and sliced into three sections to reveal the interior of the scaffold. Size bars represent (A) 2 mm, (B) 50 μ m, (C) 20 μ m, (D–F) 50 μ m.

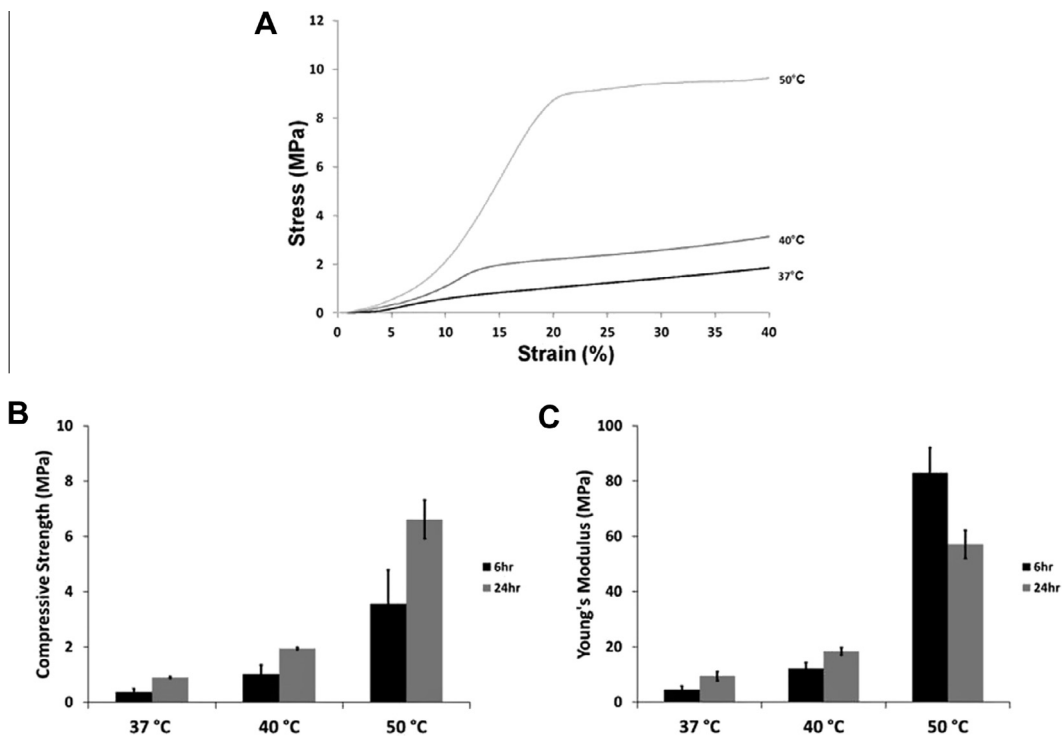


Fig. 4. Mechanical properties of scaffolds. Scaffolds were fabricated with EtOH–NaOH-treated porous PLGA microspheres for 6 h and 24 h at 37 °C, 40 °C and 50 °C. (A) Representative stress–strain graphs obtained during compression after 24 h at 37 °C. (B) Compressive strength of scaffolds sintered at 37 °C, 40 °C and 50 °C (values taken at 20% strain). (C) Young's modulus values for scaffolds sintered at 37 °C, 40 °C and 50 °C.

increasing after 6 h incubation from 4.6 ± 1.2 MPa at 37 °C to 12.2 ± 2.2 MPa at 40 °C and 83.0 ± 9.1 MPa at 50 °C. Young's modulus values also increased after 24 h incubation from 9.4 ± 1.2 MPa at 37 °C to 18.4 ± 1.3 MPa at 40 °C and 57.1 ± 5.1 MPa at 50 °C. Scaffolds were fabricated at 37 °C (body temperature) for further experiments, as this is the temperature that the microspheres would experience in clinical use.

3.4. Porosity and pore diameter of scaffolds fabricated with porous PLGA microspheres

Scaffolds were fabricated at body temperature (37 °C) for porosity and pore diameter analysis using μ CT, performed as described in Section 2.8 to assess scaffold porosity, average pore diameter and pore diameter distribution. Reconstruction images of the

scaffolds in 3-D were created in order to visualize the scaffold microstructure, as shown in Fig. 5A. Pore diameters are represented in green, varying in intensity from dark (small pores) to light green (large pores) throughout the scaffold (Fig. 5B). The average overall porosity of the scaffolds was measured at 81.6%, with a mean pore diameter of $54 \pm 38 \mu\text{m}$ and a mean maximum pore diameter of $306 \pm 79 \mu\text{m}$ (Fig. 5C). Mean maximum pore diameter was calculated by averaging the maximum pore diameter of all the scaffolds tested.

3.5. Cell attachment and proliferation on scaffolds

The 3T3 fibroblast cells were seeded onto scaffolds, as described in Section 2.10. Cell viability was assessed 3, 6 and 9 days post-seeding, using the PrestoBlue viability assay (Fig. 6A). Viable cell numbers increased significantly over time on the scaffolds, from 1.02×10^5 cells on day 3 to 2.32×10^5 on day 6 and 4.19×10^5 on day 9. Toluidine blue staining was performed on day 7, which allowed cell attachment and spreading throughout the scaffold to be visualized (Fig. 6B). Cell attachment to individual microspheres could be observed in the higher magnification images. Attachment of the red fluorescent protein-3T3 cells throughout the scaffold and to individual microspheres could also be visualized on day 14, using fluorescent microscopy as shown in Fig. 6C. By day 21, the cells were observed covering the scaffold surface in SEM images (Fig. 6D).

4. Discussion

Injectable scaffold systems have numerous advantages for use in regenerative medicine, including their ability to be delivered via a minimally invasive procedure. Although polymer microspheres have shown promise as cell delivery systems in this area, their lack of macro-porosity and mechanical strength upon injection into the body is a serious drawback for their use in repair of tissues such as bone. One method of increasing the porosity of

the delivery system is to introduce porosity into the microspheres themselves during the manufacturing process. Injectable cell delivery systems based on porous microspheres have recently been described using materials such as TCP and PLGA/HA/calcium blends [18,19]. Although such systems have proved useful as cell carriers, the microspheres do not fuse together in situ to form a scaffold that will provide macro-porosity and structural support for tissue repair. In addition, the small size of discrete microspheres can limit the ability of both the microspheres themselves and the cells they are delivering to be retained locally at the desired anatomical site following injection.

In the current study, porous PLGA microspheres were fabricated for use as an injectable scaffold material in tissue engineering applications. Non-porous PLGA microspheres of a similar size range have previously been demonstrated to be injectable through a 22G needle [12]. The use of PBS in the internal aqueous phase generated hollow microspheres with surface pores in the study described herein. The pores were further revealed through treatment with EtOH–NaOH. A treatment time of 2 min was identified as optimal for increasing porosity without compromising the structural integrity of the microspheres, as surface cracks and morphological changes occurred in microspheres treated for 3.5 and 5 min. This could be attributed to the ethanol causing the microspheres to swell, which has previously been reported with PLGA microspheres, along with collapse of surface pores by fusion of the surrounding matrix [21]. EtOH–NaOH treatment did not significantly alter microsphere average diameter ($81 \pm 26 \mu\text{m}$, $84 \pm 24 \mu\text{m}$, $81 \pm 24 \mu\text{m}$ and $82 \pm 24 \mu\text{m}$ for 0, 2, 3.5 and 5 min treatment, respectively).

The microspheres used in this study were fabricated with PLGA that has a T_g of $\sim 50^\circ\text{C}$, and therefore at the lower temperature of 37°C the microspheres would be expected to remain solid and not become cohesive. However, EtOH–NaOH-treated microspheres were able to fuse together at 37°C , unlike non-treated microspheres, indicating that polymer chains at the surface were above their T_g and able to interact with neighbouring particles. A possible explanation for this behaviour is a selective lowering of polymer

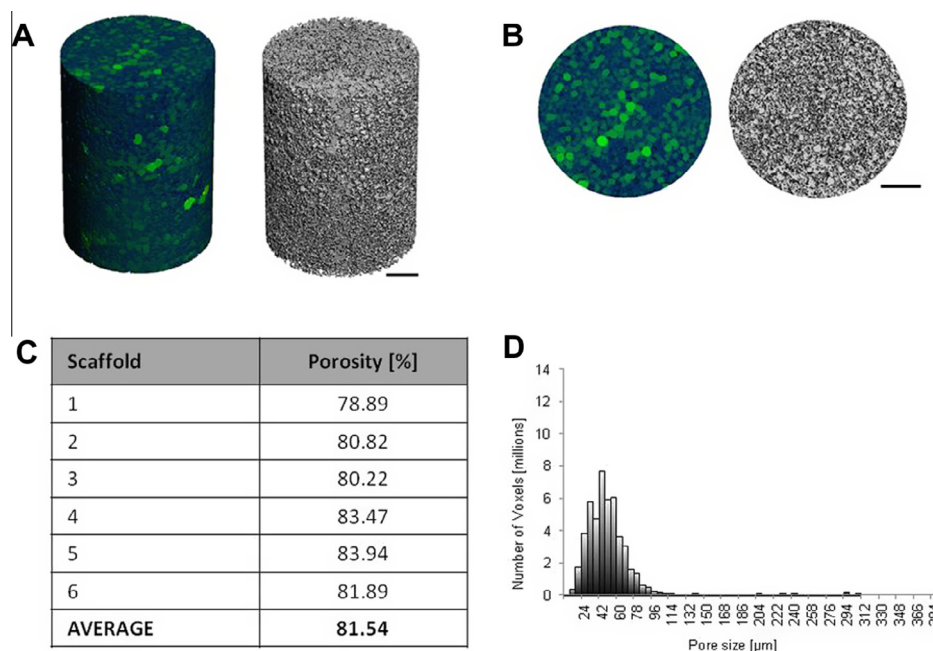


Fig. 5. Microstructural analysis of scaffolds fabricated with porous microspheres. Scaffolds were fabricated at 37°C for 24 h prior to analysis by μCT . (A) Side view 3-D reconstruction image in colour (where green areas represent air space (pores) varying in intensity from dark to light green) and greyscale. (B) Top view 3-D reconstruction image in colour and greyscale. (C) Scaffold porosity. (D) Representative pore size distribution throughout a scaffold. Size bars represent $500 \mu\text{m}$.

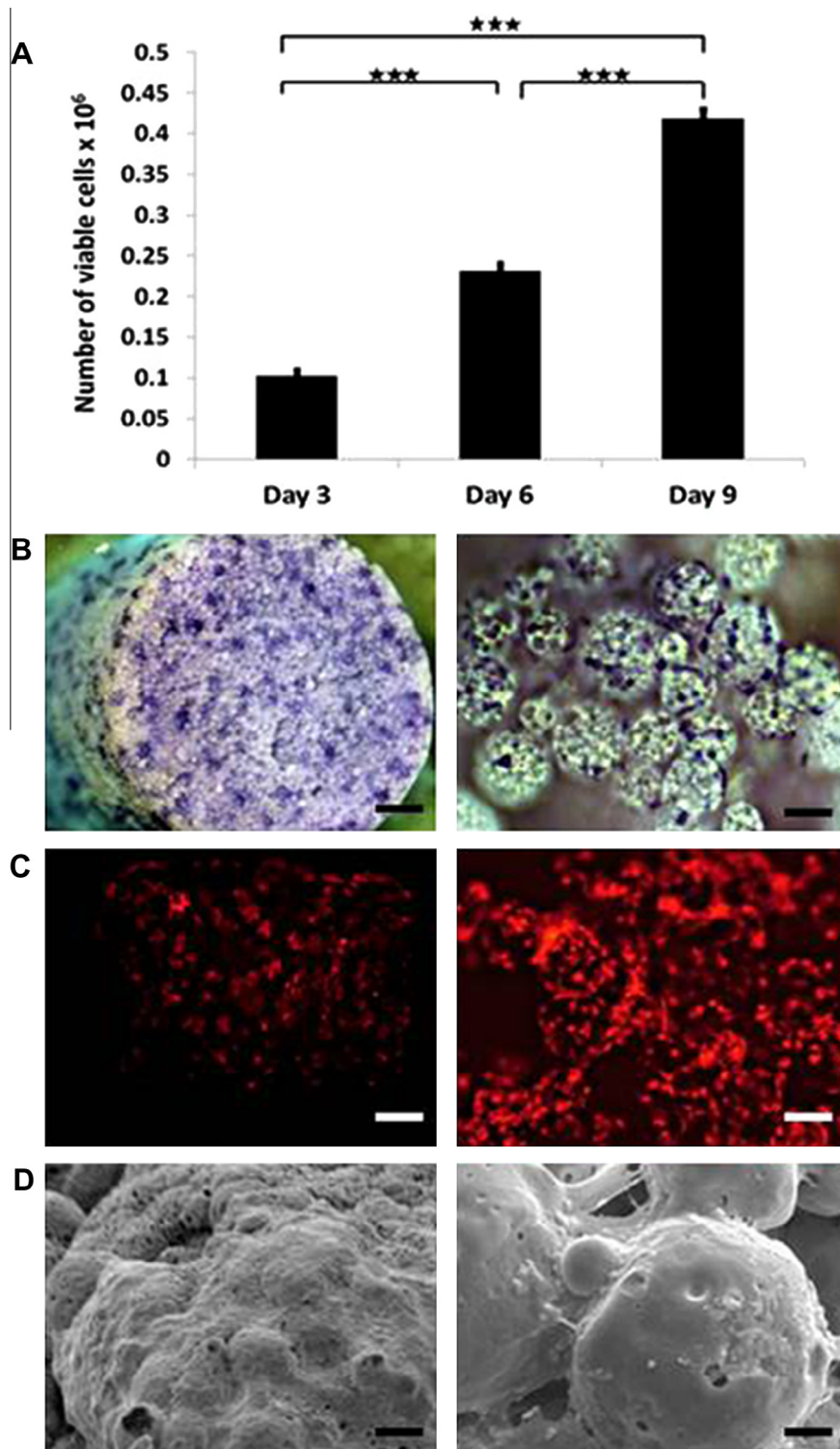


Fig. 6. Cell attachment and proliferation on scaffolds. (A) Number of viable 3T3 fibroblast cells measured by the Prestoblu metabolic activity on day 3, 6 and 9 post-seeding. (B) Bright-field microscopy images of toluidine blue stained cell-seeded scaffolds 7 days post-seeding. (C) Fluorescence microscopy images of red fluorescent 3T3 fibroblast cells 14 days post seeding. (D) SEM micrographs of cell-seeded scaffolds 21 days post-seeding.

molecular weight at the surface of EtOH–NaOH-treated microspheres as a result of hydrolysis. Measurement of bulk T_g by differential scanning calorimetry and rheology did not detect any difference in T_g in microspheres irrespective of treatment and, therefore, any reduction in T_g must be restricted to the surface of the microspheres. Microsphere fusing at four different temperatures (21 °C, 37 °C, 40 °C and 50 °C) was used as an indirect

assessment of changes in surface T_g . Microspheres did not sinter into solid scaffold structures at 21 °C, as they had not reached their T_g , but microspheres sintered into scaffold structures at 37 °C, 40 °C and 50 °C. Although scaffolds do form at 37 °C, they possess lower compressive strength on average (0.9 ± 0.1 MPa after 24 h) compared with scaffolds sintered at 40 °C (1.9 ± 0.3 MPa) and 50 °C (6.6 ± 1.2 MPa). The increase in compressive strength and

stiffness of the scaffolds as the sintering temperature was raised indicated that the microspheres were able to fuse together more as the temperature was raised closer to the PLGA glass transition temperature (50 °C).

Overall porosity level and pore diameter range are critical properties of a biomaterial scaffold. They play a vital role in tissue formation, as they allow migration and proliferation of cells into the scaffold structure as well as supporting vascularization [26]. Higher levels of porosity have been reported to enhance bone ingrowth in vivo [27]. In addition, a porous surface improves mechanical interlocking between the implant biomaterial and the surrounding tissue, providing greater mechanical stability at this critical interface [28]. Scaffolds for tissue repair ideally require both micro-porosity (pore diameters of <20 µm) and macro-porosity (pore diameters of >100 µm) [9]. The injectable scaffolds described herein possess a mean pore diameter of 54 ± 38 µm. Many injectable scaffolds are hydrogel-based and therefore often lack the micro- and macro-porosity optimal for cell migration and proliferation. Solid scaffolds can be engineered with varying levels of porosity, but these are usually preformed and therefore must be implanted. For example, implantable porous scaffolds developed from PLGA microspheres can be fabricated at 49 °C, with porosity levels ranging from 66 to 74% [29]. PLGA has been used in an injectable format when dissolved in a solvent such as tetraglycol, and injectable scaffolds of 72% average porosity have been created using such a system [17]. However, in addition to the solvent leaching out from the formulation in situ, the scaffolds displayed a relatively low average compressive strength of 0.1 MPa [17].

A delicate balance is required in terms of mechanical properties and porosity in scaffold systems, as increasing the porosity of a scaffold commonly results in a subsequent decrease in compressive strength. For example, porous PLGA scaffolds have been developed with relatively high compressive strength compared with the present system, such as scaffolds prepared from PLGA–TiO₂ microspheres, which displayed average compressive strength values of 4.8 MPa [30]. However, such scaffolds displayed comparatively lower porosity ranging from 30 to 40%. The present authors previously reported the fabrication of scaffolds for bone regeneration using non-porous PLGA/poly(ethylene glycol) (PEG) microparticles that can be either implanted or injected and solidify at 37 °C. Although they display higher compressive strength and Young's modulus values than the system described herein (2 MPa and 40 MPa, respectively, after 2 h at 37 °C), the scaffolds produced using this formulation had lower overall porosity with an average of ~40% [31]. It is clear that attaining a suitable balance between porosity and strength in an injectable scaffold formulation is a considerable challenge.

In addition to possessing suitable physical properties to support tissue regeneration, scaffolds must also be capable of facilitating cell delivery. In this regard, cell adhesion to the biomaterial is crucial for cell survival, proliferation and eventual differentiation into a specific cell type. Although PLGA has been extensively investigated in tissue engineering scaffolds, this material does have some drawbacks with regard to cell adhesion caused by its high hydrophobicity. In order to improve cell attachment, researchers have employed methods of modifying the surface of the PLGA, such as pre-coating PLGA microspheres with the adhesion molecules of RGD peptide, or treating microspheres with plasma polymerized allylamine [12,13,32]. In the current study, PLGA microspheres were not directly treated to enhance cell attachment, but they were treated with EtOH–NaOH to increase surface porosity. As described in Section 2.9, the 3T3 fibroblast cell suspension was mixed with microspheres using a spatula, and the resulting paste was packed into a mould, which was transferred to a sealed humidified chamber containing DMEM at 37 °C. After 24 h, scaffolds were removed from mould, transferred into 12-well cell

culture plates with fresh medium and incubated at 37 °C. The ability of the cells to attach to and proliferate on the microspheres within the scaffolds following the fabrication process was assessed. Viable cell number increased over time in culture from 1×10^5 cells per scaffold on day 3 to 4×10^5 on day 9, demonstrating proliferation of the 3T3 cells over the 9-day time period. Cell attachment was visualized on the scaffolds using toluidine staining and fluorescence microscopy, with cells appearing to attach well to the microspheres within the scaffolds and to spread over the scaffold structure. An increase in the number of attached cells was observed over time in culture, culminating with a monolayer of cells covering the particles by day 21. NIH-3T3 fibroblasts have previously been shown to attach and proliferate on injectable porous PLGA microspheres 535 µm in size, with surface pores up to 20 µm, fabricated using ammonium bicarbonate as a porogen, but these microspheres did not form scaffolds in situ [33]. Future work will investigate the ability of the injectable scaffold system described in this study to deliver viable cells and regenerate tissue in vivo.

5. Conclusion

In this study, hollow, porous PLGA microspheres were developed, which fuse together at 37 °C to form highly porous scaffold structures in situ that support cell attachment and proliferation. To the best of the present authors' knowledge, this is the first demonstration of the use of porous PLGA microspheres that physically fuse together without the use of solvents at body temperature as an injectable scaffold system. This technology is a promising minimally invasive approach formation of porous biodegradable scaffolds in situ for tissue repair applications.

Disclosures

There are no potential conflicts of interest to disclose for this work.

Acknowledgments

This work was funded by the European Community's FP7 project Bidesign EUPF7-NMP.20102.3-1 (grant: 262948) and the European Research Council under the European Community's Seventh FP7 project FP72007-2013 (grant: 227845). The authors would also like to thank Dr. James Dixon (University of Nottingham) for kindly providing the red fluorescent labelled NIH-3T3 cells.

References

- [1] Mooney DJ, Vandenburgh H. Cell delivery mechanisms for tissue repair. *Cell Stem Cell* 2008;2:205–13.
- [2] Yang S, Leong KF, Du Z, Chua CK. The design of scaffolds for use in tissue engineering. Part I. Traditional factors. *Tissue Eng* 2001;7:679–89.
- [3] Jiang T, Abdel-Fattah WI, Laurencin CT. In vitro evaluation of chitosan/poly(lactic acid-glycolic acid) sintered microsphere scaffolds for bone tissue engineering. *Biomaterials* 2006;27:4894–903.
- [4] White LJ, Kirby GTS, Cox HC, Qodratnama R, Qutachi O, Rose FRAJ, et al. Accelerating protein release from microparticles for regenerative medicine applications. *Mater Sci Eng C Mater Biol Appl* 2013;33:2578–83.
- [5] Ren T, Ren J, Jia X, Pan K. The bone formation in vitro and mandibular defect repair using PLGA porous scaffolds. *J Biomed Mater Res A* 2005;74A:562–9.
- [6] Rahman CV, Ben-David D, Dhillon A, Kuhn G, Gould TW, Muller R, et al. Controlled release of BMP-2 from a sintered polymer scaffold enhances bone repair in a mouse calvarial defect model. *J Tissue Eng Regen Med* 2012;8:59–66.
- [7] Curran JM, Fawcett S, Hamilton L, Rhodes NP, Rahman CV, Alexander M, et al. The osteogenic response of mesenchymal stem cells to an injectable PLGA bone regeneration system. *Biomaterials* 2013;34:9352–64.
- [8] Kirby GTS, White LJ, Rahman CV, Cox HC, Qutachi O, Rose FRAJ, et al. PLGA-based microparticles for the sustained release of BMP-2. *Polymers* 2011;3:571–86.

- [9] Bose S, Roy M, Bandyopadhyay A. Recent advances in bone tissue engineering scaffolds. *Trends Biotechnol* 2012;30:546–54.
- [10] Murphy CM, O'Brien FJ, Little DG, Schindeler A. Cell-scaffold interactions in the bone tissue engineering triad. *Eur Cell Mater* 2013;26:120–32.
- [11] Bhat A, Dreifke MB, Kandimalla Y, Gomez C, Ebraheim NA, Jayasuriya AC. Evaluation of cross-linked chitosan microparticles for bone regeneration. *J Tissue Eng Regen Med* 2010;4:532–42.
- [12] Bible E, Chau DY, Alexander MR, Price J, Shakesheff KM, Modo M. Attachment of stem cells to scaffold particles for intra-cerebral transplantation. *Nat Protoc* 2009;4:1440–53.
- [13] Bible E, Chau DY, Alexander MR, Price J, Shakesheff KM, Modo M. The support of neural stem cells transplanted into stroke-induced brain cavities by PLGA particles. *Biomaterials* 2009;30:2985–94.
- [14] Bible E, Qutachi O, Chau DY, Alexander MR, Shakesheff KM, Modo M. Neovascularization of the stroke cavity by implantation of human neural stem cells on VEGF-releasing PLGA microparticles. *Biomaterials* 2012;33:7435–46.
- [15] Kawai K, Suzuki S, Tabata Y, Ikada Y, Nishimura Y. Accelerated tissue regeneration through incorporation of basic fibroblast growth factor-impregnated gelatin microspheres into artificial dermis. *Biomaterials* 2000;21:489–99.
- [16] Kang S-W, La W-G, Kim B-S. Open macroporous poly(lactic-co-glycolic acid) microspheres as an injectable scaffold for cartilage tissue engineering. *J Biomater Sci Polym Ed* 2009;20:399–409.
- [17] Krebs MD, Sutter KA, Lin ASP, Guldberg RE, Alsberg E. Injectable poly(lactic-co-glycolic) acid scaffolds with in situ pore formation for tissue engineering. *Acta Biomater* 2009;5:2847–59.
- [18] Cheng D, Gao H, Hao L, Cao X, Wang Y. Facile development of a hollow composite microsphere with porous surface for cell delivery. *Mater Lett* 2013;111:238–41.
- [19] Ryu T-K, Oh M-J, Moon S-K, Paik D-H, Kim S-E, Park J-H, et al. Uniform tricalcium phosphate beads with an open porous structure for tissue engineering. *Colloids Surf B: Biointerfaces* 2013;112:368–73.
- [20] Yang Y, Bajaj N, Xu P, Ohn K, Tsifansky MD, Yeo Y. Development of highly porous large PLGA microparticles for pulmonary drug delivery. *Biomaterials* 2009;30:1947–53.
- [21] Kim HK, Chung HJ, Park TG. Biodegradable polymeric microspheres with "open/closed" pores for sustained release of human growth hormone. *J Control Rel* 2006;112:167–74.
- [22] Gao J, Niklason L, Langer R. Surface hydrolysis of poly(glycolic acid) meshes increases the seeding density of vascular smooth muscle cells. *J Biomed Mater Res* 1998;42:417–24.
- [23] Hildebrand T, Laib A, Müller R, Dequeker J, Rügsegger P. Direct three-dimensional morphometric analysis of human cancellous bone: microstructural data from spine, femur, iliac crest, and calcaneus. *J Bone Miner Res* 1999;14:1167–74.
- [24] van Lenthe GH, Hagenmüller H, Bohner M, Hollister SJ, Meinel L, Müller R. Nondestructive micro-computed tomography for biological imaging and quantification of scaffold–bone interaction in vivo. *Biomaterials* 2007;28:2479–90.
- [25] Dixon JE, Dick E, Rajamohan D, Shakesheff KM, Denning C. Directed differentiation of human embryonic stem cells to interrogate the cardiac gene regulatory network. *Mol Ther* 2011;19:1695–703.
- [26] Kuboki Y, Takita H, Kobayashi D, Tsuruga E, Inoue M, Murata M, et al. BMP-induced osteogenesis on the surface of hydroxyapatite with geometrically feasible and nonfeasible structures: topology of osteogenesis. *J Biomed Mater Res* 1998;39:190–9.
- [27] Karageorgiou V, Kaplan D. Porosity of 3D biomaterial scaffolds and osteogenesis. *Biomaterials* 2005;26:5474–91.
- [28] Story BJ, Wagner WR, Gaisser DM, Cook SD, Rust-Dawicki AM. In vivo performance of a modified CSTI dental implant coating. *Int J Oral Maxillofac Implants* 1998;13:749–57.
- [29] Clark A, Milbrandt TA, Hilt JZ, Puleo DA. Mechanical properties and dual drug delivery application of poly(lactic-co-glycolic acid) scaffolds fabricated with a poly(β -amino ester) porogen. *Acta Biomater*. 2014;10:2125–32.
- [30] Wang Y, Shi X, Ren L, Yao Y, Zhang F, Wang D-A. Poly(lactide-co-glycolide)/titania composite microsphere-sintered scaffolds for bone tissue engineering applications. *J Biomed Mater Res B: Appl Biomater* 2010;93B:84–92.
- [31] Rahman CV, Kuhn G, White LJ, Kirby GTS, Varghese OP, McLaren JS, et al. PLGA/PEG-hydrogel composite scaffolds with controllable mechanical properties. *J Biomed Mater Res B: Appl Biomater* 2013;101B:648–55.
- [32] Park JS, Yang HN, Jeon SY, Woo DG, Na K, Park KH. Osteogenic differentiation of human mesenchymal stem cells using RGD-modified BMP-2 coated microspheres. *Biomaterials* 2010;31:6239–48.
- [33] Kim TK, Yoon JJ, Lee DS, Park TG. Gas foamed open porous biodegradable polymeric microspheres. *Biomaterials* 2006;27:152–9.